A pilot study on saccadic adaptation experiments with robots

Eris Chinellato[1], Marco Antontelli[2], and Angel P. del Pobil[2]

[1] Imperial College London, South Kensington Campus, London SW7 2AZ, UK
e.chinellato@imperial.ac.uk
[2] Jaume I University, Campus Riu Sec, 12071, Castellón de la Plana, Spain
{antonell,pobil}@icc.uji.es

Abstract. Despite the increasing mutual interest, robotics and cognitive sciences are still lacking common research grounds and comparison methodologies, for a more efficient use of modern technologies in aid of neuroscience research. We employed our humanoid robot for reproducing experiments on saccadic adaptation, on the same experimental setup used for human studies. The behavior of the robot, endowed with advanced sensorimotor skills and high autonomy in its interaction with the surrounding environment, is based on a model of cortical sensorimotor functions. We show how the comparison of robot experimental results with human and computational modeling data allows researchers to validate and assess alternative models of psychophysical phenomena.

1 Introduction

Artificial intelligence has been from its very foundation a meeting-place for scientists of seemingly unrelated disciplines. The impact of interdisciplinary research involving high technology fields and life sciences is now growing faster and faster. Two disciplines which met thanks to artificial intelligence are robotics and neuroscience, and their encounter is producing mutually beneficial developments. For example, bio-mimetic robotics constitutes an important way for technological improvement, while representing a scientific advancement toward the understanding of how biological systems work. The research of common grounds on which to pursue an effective cross-fertilization is not new [9, 10, 14], and concrete proposals have been put forth in order to facilitate communication and interchange between roboticists and neuroscientists [3, 5, 17]. Still, fundamental differences in research goals, methodologies and language prevent a more proficuous collaboration between the fields.

With this work we provide a new contribution to the above goals, by training a humanoid robot to perform simulated psychophysical experiments. The behavior of the robot is based on a model designed with the purpose of achieving visuomotor awareness of the environment by using eye and arm movements [4]. The implementation of the model on the humanoid robot provides it with the capability of performing concurrent or decoupled gazing and reaching movements toward visual or memorized targets placed in its peripersonal space [1]. In this

paper we check the robot skills on an experimental setup resembling those used in human psychophysical studies. On the one hand, these tests allow to validate the underlying properties of the computational model on which the robot behavioral abilities are built upon. On the other hand, we wish to verify if our robotic system can represent a research tool able to emulate human experiments, and thus constitute a potential aid in the design and analysis of actual experimental protocols. Simulating psychophysical experiments on the robot can be useful to check in advance the appropriateness of experimental protocols, reducing the expensive and complicated preliminary tests with human subjects [8].

We present here a benchmark test for our proposal, which also constitutes the first theoretical contribution of our system towards the study of eye gazing mechanisms in humans. To achieve such a goal we present our robot with a cognitive science experimental setup similar to those used for saccadic adaptation experiments in humans [7, 16]. The comparison of human experimental data with a computational simulation and with the robot tests provide insights on theoretical aspects related to visuomotor cognitive aspects, and contextually allows us to validate our model.

In the next Section 2 we describe how saccadic adaptation experiments are normally executed with human subjects and their typical outcome, and how we built our robotic system in order to be able to replicate such experiments with a humanoid robot. Section 3 describes the experimental setup and the outcome of both simulated and actual robot experiments, which are compared and discussed in Section 4.

2 Saccadic adaptation in humans and robots

2.1 Saccadic adaptation in humans

The phenomenon of saccadic adaptation can be observed when the visual feedback provided to a subject after an eye movement is inconsistent with the location of the target before the movement (see Fig. 1(a), which will be described with more detail in Section 3). In these conditions, the subject gradually learns to perform a saccadic movement that allows her to fixate the expected final position of the stimulus, even though this is displaced with respect to its initial position [12]. Saccadic adaptation experiments can be either inward, when the target is displaced toward the starting point, thus causing a reduction of the saccadic movement amplitude, or outward, when the target is displaced further away from the starting point, thus causing larger saccadic movements. Saccadic adaptation is not limited to the point of adaptation, but transfers to the nearby visual space. Amplitude of post-adaptation saccades on stimuli around the adapted target varies according to the distance and the relative position with respect to the target point, a phenomenon called adaptation transfer.

The reference graphs for human experiments are reproduced in Fig. 2, above for the inward protocol [7], below for the outward protocol [16]. For both cases three fundamental aspects are analyzed, the same that we will explore in our experiments. Fig. 2(a) and 2(d) show the adaptation trend, i.e. the time course of

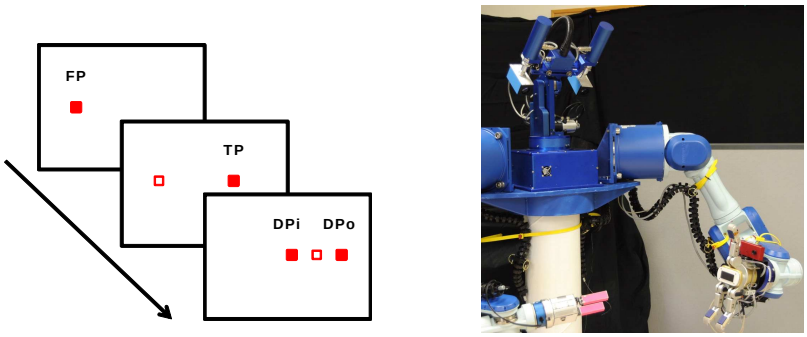

(a) Experimental protocol (b) Humanoid robot

Fig. 1. Experimental protocol (filled squares represent currently visual stimuli, empty squares are disappeared stimuli) and humanoid robot with pan/tilt/vergence head.

the gradual shift of the subject response from the initial movement amplitude to the displaced target, for inward and outward adaptation respectively. Saccadic adaptation fields, displayed in Fig. 2(b) and 2(e), are a local representation of adaptation transfer, assessing how the mis-trained movement affects saccades directed towards different targets in space. Black dots represent movement average endpoint before adaptation, while the end of the segments represent the average endpoint after adaptation. Finally, adaptation transfer accumulated along the fundamental axes is visualized in Fig. 2(c) and 2(f), where the horizontal (x) and vertical (y) components of the displacements of the adaptation field are represented separately as a function of the x coordinate.

2.2 The model and the humanoid robot implementation

Our humanoid robot system was designed with the goal of achieving advanced capabilities in the interaction of an autonomous system with its nearby environment. To this purpose, we conceived and implemented a sensorimotor framework composed of three Radial Basis Function Networks (see Fig. 3, details can be found in [4]): one for converting the visual position of a stimulus into an oculomotor position (left transformation block in the diagram), and the other two for hand-eye movement coordination (right transformation block). Networks of suitable basis functions are able to naturally reproduce the gain-field effects often observed in parietal neurons and are particularly suitable for maintaining sensorimotor associations [15]. We have designed our computational schema and the neural networks which compose it directly from insights drawn from the analysis of monkey single-cell data on reaching and gazing experiments registered from posterior parietal area V6A [2, 6].

Similarly to the way primates explore their environment, in our framework the robot incrementally builds a sensorimotor representation of the peripersonal space, through subsequent, increasingly complex interactions composed by sequences of saccades and reaching movements [1, 4]. As a first step, the system

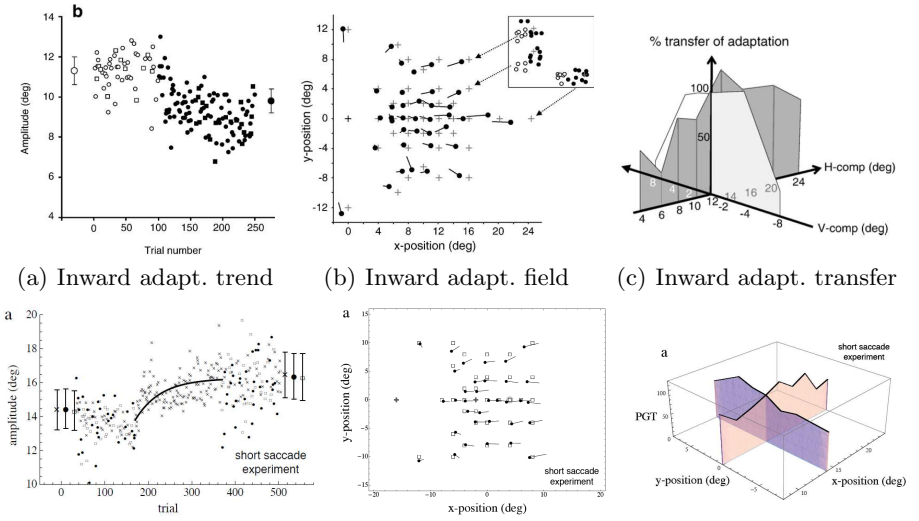

(a) Inward adapt. trend (b) Inward adapt. field (c) Inward adapt. transfer

(d) Outward adapt. trend (e) Outward adapt. field (f) Outward adapt. transfer

Fig. 2. Human saccadic adaptation results for inward (above, from [7]) and outward adaptation experiments (below, from [16]).

learns to associate retinal information and gaze direction (i.e. proprioceptive eye position), using successive foveation movements to salient points of the visual space. This allows to create a mapping, performed by the first neural network, between visual information and oculomotor (vergence - version) coordinates. Gaze direction is then associated to arm position, by moving the arm randomly and following it with the gaze, so that each motor configuration of the arm joints is associated to a corresponding configuration of the eye motor control, and vice versa. This process allows the robot to learn the bidirectional link between different sensorimotor systems, so that it can look where its hand is but also reach the point in space it is looking at. Hence, the representation of the peripersonal space is maintained contextually by both limb sensorimotor signals on the one hand and by visual and oculomotor signals on the other hand.

The described learning framework endows the robot with the ability of exploring and building an egocentric representation of its surrounding environment, through the execution of coupled or decoupled gazing and arm reaching actions, on either visible or memorized targets. Whilst the above skills have been described in previous works [1, 4], we introduce in this paper a novel scenario, in which the robot visual environment is constituted by a computer screen placed right in front of it, on which small geometrical shapes are visualized. This scenario corresponds to the typical setup of psychophysical experiments on humans and other primates, and we present it here to the robot in order to engage it in saccadic adaptation experiments similar to those typically performed on human subjects.

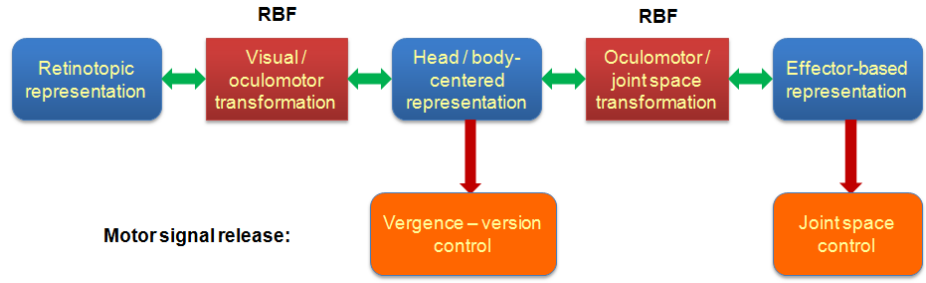

Fig. 3. Computational model for building a visuomotor awareness of the environment through gazing and reaching movements.

3 Experimental evaluation

The typical psychophysics experimental setup on which the skills of our humanoid robot are tested consists of a computer screen placed within reaching distance, visualizing different visual stimuli associated to action signals. It is worthwhile to clarify that, although vergence varies very little in this setup, all transformations are fully tridimensional, and the robot keeps acting as in the usual 3D configuration. On the other hand, as these experiments require no arm movements, only the visual to oculomotor neural network is involved in this study. Details on the experimental setup are provided below.

3.1 Experimental Setup

Our robot is a humanoid torso endowed with a pan-tilt-vergence stereo head and two multi-joint arms (Fig. 1(b)). The head mounts two cameras separated by a 270mm baseline, and having a resolution of 1024x768 pixels that can acquire color images at 30 Hz. After the RBFNs underlying the robot behavior have been trained, saccadic adaptation experiments are performed according to the protocol described below (see Fig. 1(a)). A computer monitor (1440x900, 19") is put in front of the robot at a distance of 720mm, which allows to obtain version angles similar to human experiments without getting too close to image periphery. The experiment program is designed to display at required positions small red squares (5x5 pixels), unambiguously identified by the robot module for blob detection.

The task begins with the robot looking straight ahead at a fixation point stimulus (FP) corresponding to null version angles (frame 1 of Fig. 1(a)). A second visual stimulus is then showed at the target position (TP), having the same vertical but different horizontal coordinate, increased by a certain amount Δx, parameter of the experiment, while FP disappears (frame 2 of Fig. 1(a)). The robot is required to perform a saccade toward this new stimulus. When the saccade movement signal is released and the robot starts moving, the stimulus is displaced toward a third point (DP), either closer (DPi) or further (DPo) on

the x axis with respect to TP (for *inward* and *outward* saccadic adaptation protocols, respectively, frame 3 of Fig. 1(a)). At the end of the movement, the robot perceives a visual error between its final position, corresponding to TP if the saccade is correctly executed, and the visible target DP. Such visual difference is used to adapt the weights of the network performing the transformation from retinal to oculomotor coordinates. The starting stimulus is then shown again and the robot saccades back toward it. The whole sequence is repeated 100 times.

Before performing the saccadic adaptation tests with the real robot, we simulated them using the robot model on a corresponding virtual setup. This simulation is useful for predicting the sort of results that experiments with the real robot are expected to provide. On the one hand, this is done to avoid keeping the robot busy with the execution of irrelevant experiments. On the other hand, it allows to assess the impact that real world tests have on the purely theoretical insights provided by the simulation.

3.2 Simulated experiments

We tested each of the two experimental protocols, inward and outward adaptation, with two different configurations of the visual to oculomotor radial basis function network. The *uniform* configuration has the centers of the basis functions distributed evenly on the input space (x and y cyclopean coordinates and horizontal disparity). In the *logarithmic* distribution neurons are placed closer to each other at the center of the visual field and for small disparities. While for the uniform distribution all neurons have the same spread, in the logarithmic case radii vary according to the distance of a neuron from its neighbors. For what concerns the parameters of the experimental setup, the target was fixed for all experiments at 11.89° on the right of the starting point, while the displaced point was set at 7.96° for inward displacements and at 15.73° for outward displacements. These values were set considering the robotic setup, in order to generate eye version movements comparable to those of human tests. The results we obtained with our simulation are shown in Fig. 4. Adaptation trend, adaptation field and adaptation transfer (columns) are depicted for: uniform inward, uniform outward, logarithmic inward and logarithmic outward tests (rows).

Adaptation trend graphs (Fig. 4(a), 4(d), 4(g) and 4(j)) show a plausible learning curve which reduces (in the inward case) or increases (in the outward case) movement amplitude according to the deceiving feedback provided by the displaced target stimulus. In the uniform distribution tests, movement amplitude gets at trial 100 to 8.79° in the inward protocol and to 14.92° in the outward protocol, from the initial 11.89°, for a final adaptation of 79.5% and 77% respectively. The average adaptation over all trials is of 2.1° in both cases, about 54% of the target step. Slightly higher values (faster adaptation) have been obtained in the logarithmic case. In general, average adaptation values for humans are smaller than what we found in our simulation. For the inward case, only a 13% adaptation was observed [7], whilst 33%-45% adaptations were registered for outward experiments [16], depending on the initial saccade amplitude.

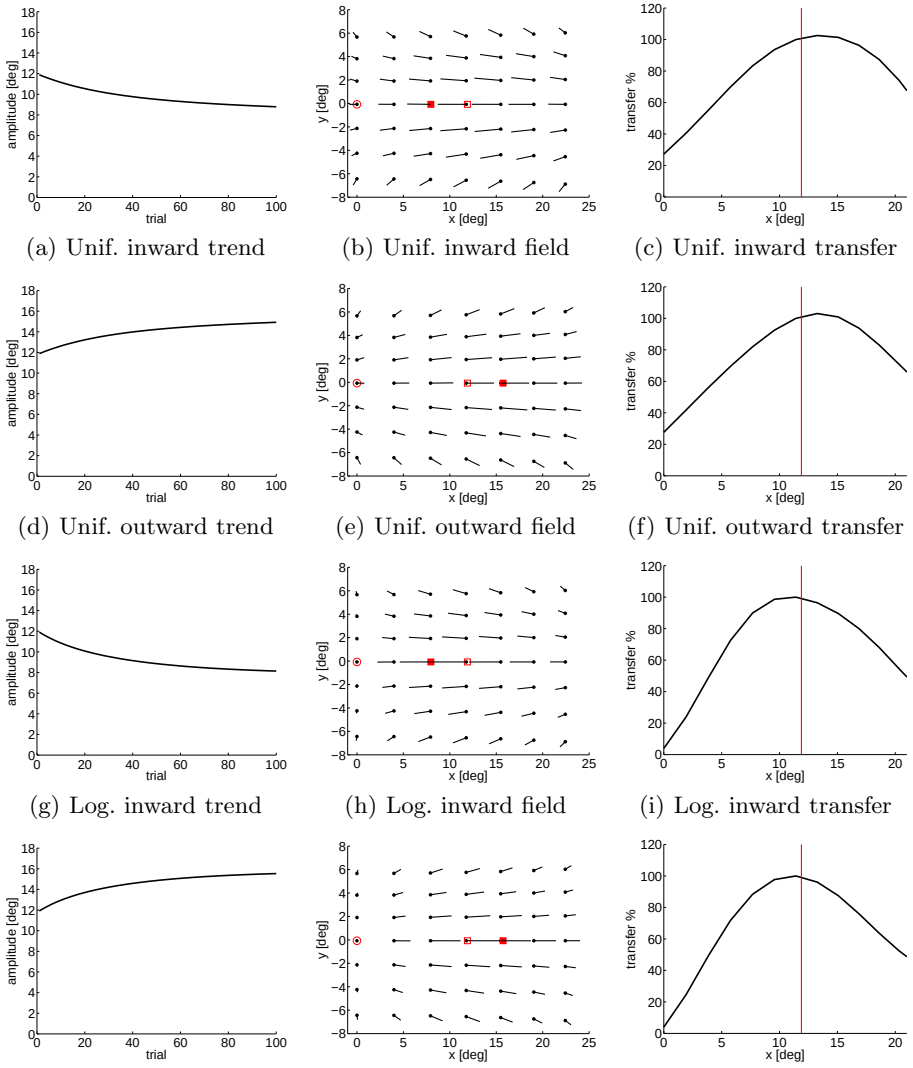

(a) Unif. inward trend (b) Unif. inward field (c) Unif. inward transfer

(d) Unif. outward trend (e) Unif. outward field (f) Unif. outward transfer

(g) Log. inward trend (h) Log. inward field (i) Log. inward transfer

(j) Log. outward trend (k) Log. outward field (l) Log. outward transfer

Fig. 4. Saccadic adaptation results for computational model, for both Uniform and Logarithmic distribution of RBFs.

Adaptation fields (Fig. 4(b), 4(e), 4(h) and 4(k)) have in all cases a perceptible radial trend, with a y component indicating wider movements toward the top or the bottom of the screen for both protocols and net configurations. This is rather consistent with Schnier and colleagues outward tests (see Fig. 2(e)), but much less apparent for what concerns inward experiments (Fig. 2(b)).

The overall trend of the adaptation over the horizontal (x) component can be observed in the adaptation transfer graphs of Fig. 4(c), 4(f), 4(i) and 4(l). Human experiments suggest that, both for input and outward adaptation (see Fig. 2(c) and Fig. 2(f)), the difference between pre- and post-adaptation movements peaks just after the abscissa of the target. Also, while transfer decreases with the distance from the peak, such decrease is slower for larger saccades than for shorter ones (gentler slopes on the right side of the peak). It seems that the uniform configuration captures the first of this phenomena, showing a peak in transfer for movement amplitudes slightly after the target. Still, the transfer is symmetrical with respect to the peak. The opposite occurs for the logarithmic distribution, which transfer peak appears slightly before the target abscissa. The transfer trend is though asymmetrical, showing a less pronounced decrease on the right of the peak. As observed in both inward and outward studies on humans, the adaptation vertical (y) component had a very small error rather homogeneous for different movement amplitudes, with no clear trend worth visualization.

3.3 Robot experiments

The same two configurations of the visual to oculomotor RBFN employed in the simulation were used also in the real robot experiments. The adopted configurations were chosen through an exhaustive search of the center locations and spreads providing the highest precision in approximating the goal function.

The network weights found on the model, and used in the simulated saccadic adaptation experiments described above, were transferred to the real robot. A short training phase with on-screen visual stimuli was then executed in order to adapt the network to possible distortions and unavoidable differences between the model and the real robot setup. This was performed by randomly showing a point on the screen, which the robot had to saccade to. The possible residual error of the movement was employed to train the network. As in the simulation, four saccadic adaptation experiments were conducted with the robot, characterized by the basic structure of the visual to oculomotor network (uniform or logarithmic distribution of the centers) and by the direction of the displacement (inward or outward). Target and displaced point were the same as above: initial target 11.89°, inward displaced point 7.96°, outward displaced point 15.73°.

All results are depicted in Fig. 5, matching the correspondent graphs of Fig. 4, obtained in the simulation for the same conditions. The adaptation trend is shown in Fig. 5(a), 5(d), 5(g) and 5(j) for the four different tests. The only noticeable difference with the simulation is a short initial sequence of trials in which the system seems to be resilient to learning the new movement amplitude, but after that the trend is very similar to what observed for the model and in human experiments. The final and average movement amplitudes are 66.5%

and 43.0% for inward and 60.5% and 40.7% for outward adaptation, respectively. These smaller values suggest that, employing the same learning rate, the robot achieves a better approximation of the human data with respect to the simulation. Again, the logarithmic network provides higher adaptation values.

To study adaptation transfer, an adaptation field was created by defining a 20x25 lattice on the screen. All points on the lattice were shown one at time, and the robot was required to perform a saccade toward each stimulus starting from FP. At the end of the movement, the visual position of the stimulus and the oculomotor angles were compared. This process was performed before and after saccadic adaptation, but could be executed at any one of the 100 steps of the experiment, in order to monitor the progress of adaptation transfer. It is important to clarify that, during this evaluation task, learning is suspended and the network is frozen in its current state. This solution allows to monitor precisely the evolution of the saccadic adaptation learning process, and constitutes thus an advantage with respect to human experiments, where such freezing is clearly not possible. Adaptation fields are shown in Fig. 5(b), 5(e), 5(h) and 5(k), in which, for clarity reasons, only a subset of the lattice points have been visualized. The radial effect, when present, is very light and not consistent across different positions, showing a pattern more similar to the human data than to the simulation results, which present a stronger radial effect.

Interesting insights can be drawn by observing the horizontal (x) component of the movement change (Fig. 5(c), 5(f), 5(i) and 5(l)). A late peak can be observed in both experiments for the uniform configuration (more pronounced than in the simulation), and for the logarithmic distribution in the inward adaptation test. Moreover, practically all cases show an asymmetry of the transfer, with curves descending more slowly for larger saccades, as it happens in the human case, whilst simulation curves are clearly symmetrical. This effect is again stronger for the logarithmic network configuration. Such slightly more plausible results achieved by the logarithmic networks is consistent with the non homogeneous distribution of the neural receptive fields in the retina and primary visual cortex. Once more, no relevant effects were observed for what concerns the vertical adaptation transfer component.

As a general consideration, it can be observed that the robot results approximate the human data better than the simulated results. The reduced radial aspect of the adaptation field and the trend of the horizontal component in peak position and slope asymmetry are more consistent between human and robot than the correspondent simulated results.

4 Discussion and Conclusion

Different properties observed in human saccadic adaptation studies were captured by our tests. Both the simulation and the robot experiments showed plausible adaptation trends, slightly radial adaptation fields and typical features of the adaptation transfer on the horizontal component, such as asymmetry and late peak. Reminding that our model is based on a direct mapping between visual

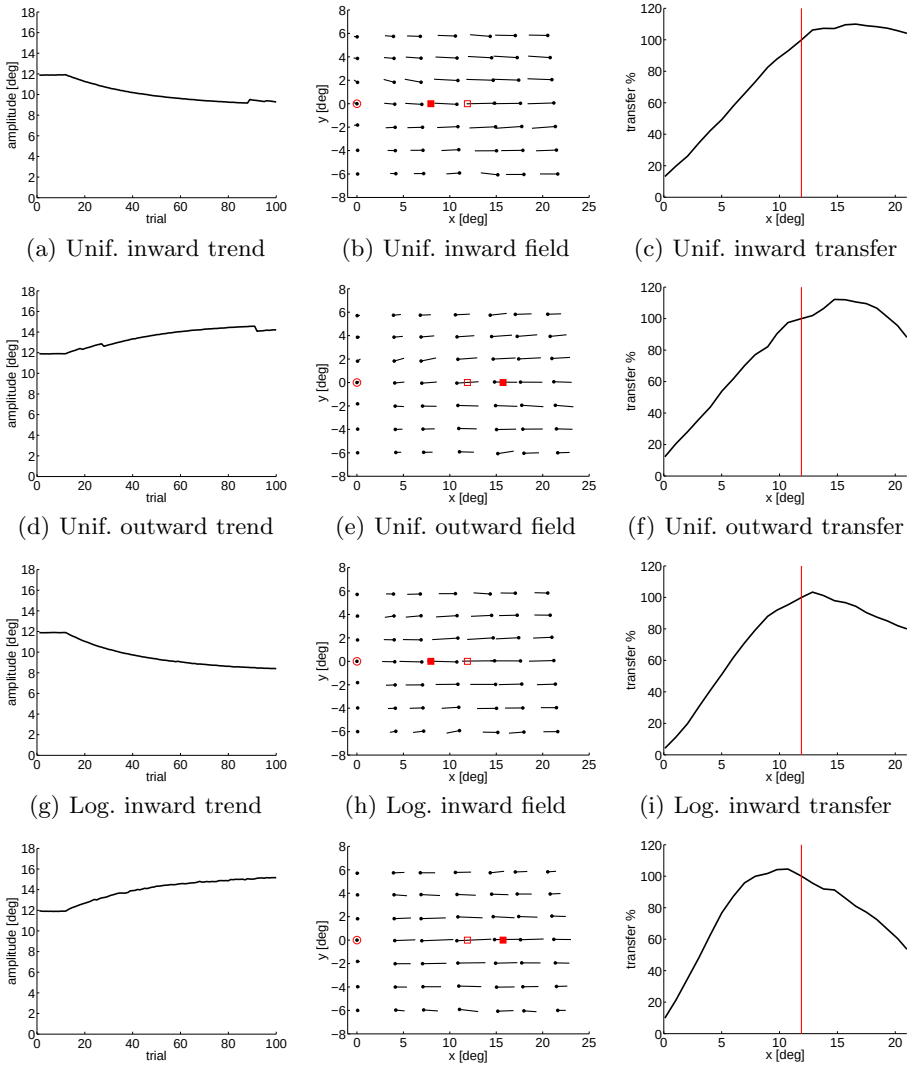

(a) Unif. inward trend (b) Unif. inward field (c) Unif. inward transfer

(d) Unif. outward trend (e) Unif. outward field (f) Unif. outward transfer

(g) Log. inward trend (h) Log. inward field (i) Log. inward transfer

(j) Log. outward trend (k) Log. outward field (l) Log. outward transfer

Fig. 5. Saccadic adaptation results for robot experiments, for both Uniform and Logarithmic distribution of RBFs.

stimuli and oculomotor signals, the above results support the view that saccadic adaptation is a multifold phenomenon related not only to motor aspects, but also to more complex cortical sensorimotor processes [11]. On this regard, the role of posterior parietal areas, and especially of area V6A on which our model was based upon, seems to be of particular interest and worth of further exploration.

From a computational point of view, it is worth highlighting that real robot experiments provided a better approximation of human data with respect to the model. This is especially interesting considering that exactly the same parameters were employed in the two cases. This phenomenon might reflect implicit properties of the embodiment that affect the way untrained movements are biased by learning processes applied to similar movements. Unmodeled aspects, such as the noise in the identification of stimulus location, might also contribute to this effect, and we are conducting further studies in order to clarify this issue. In any case, the phenomenon represents a rationale supporting robot emulation of psychophysical experiments as preferable to computational simulations.

Abstracting from the study case of saccadic adaptation analyzed in this work, having humanoid robots performing psychophysical experiments represents an important common tool for robotics and cognitive sciences. We can use robot experiments for comparing, and validate, possible explanations of experimental results deriving from different models. Moreover, the rigorous model design required by actual robotic implementation is likely to represent an ideal environment on which to devise more detailed and plausible models, and can be an inspiration source for planning completely new experiments.

There is an additional important advantage that we plan to achieve through our system, which is, the possibility of performing "impossible experiments". In fact, many neuroscientific theories derive from observations done on neurally-impaired people. Such experiments cannot be reproduced, neither it is possible to decide beforehand the type of brain damage on which to investigate, but they can be tested on a robot system on which some modules have been damaged or important parameters altered. In this regard, we are planning to assess the effect of saccadic adaptation on arm movements, to verify how a visuomotor phenomenon transfers to other motor domains. We can do this by artificially altering the parameters of the model on which the oculomotor to arm-motor transformation is performed, and verifying if and how this affect reaching movements in the saccadic adaptation paradigm (see e.g. [13]).

Acknowledgments

This work was supported by the National Research Foundation of Korea (WCU program) funded by the Ministry of Education, Science and Technology (Grant R31-2008-000-10062-0), by the Spanish Ministerio de Ciencia e Innovación (FPI Grant BES-2009-027151 and DPI2011-27846), by Generalitat Valenciana (PROMETEO/2009/052) and by Fundació Caixa Castelló-Bancaixa (P1-1B2011-54).

The authors would like to thank Markus Lappe for many helpful discussions and advice regarding the experiments and earlier drafts of this paper.

References

1. M. Antonelli, E. Chinellato, and A.P. del Pobil. Implicit mapping of the peripersonal space of a humanoid robot. In *IEEE Symposium Series on Computational Intelligence - SSCI*, 2011.
2. A. Bosco, R. Breveglieri, E. Chinellato, C. Galletti, and P. Fattori. Reaching activity in the medial posterior parietal cortex of monkeys is modulated by visual feedback. *J. Neurosci*, 30(44):14773–14785, 2010.
3. G. Cheng, Sang-Ho Hyon, J. Morimoto, A. Ude, G. Colvin, W. Scroggin, and S. C. Jacobsen. Cb: A humanoid research platform for exploring neuroscience. In *Proc. 6th IEEE-RAS Int Humanoid Robots Conf*, pages 182–187, 2006.
4. E. Chinellato, M. Antonelli, B.J. Grzyb, and A.P. del Pobil. Implicit sensorimotor mapping of the peripersonal space by gazing and reaching. *IEEE Transactions on Autonomous Mental Development*, 3(1):43–53, 2011.
5. E. Chinellato and A. P. del Pobil. fRI, functional robotic imaging: Visualizing a robot brain. In *IEEE International Conference on Distributed Human-Machine Systems DHMS*, Athens, Greece, March 2008.
6. E. Chinellato, B. J. Grzyb, N. Marzocchi, A. Bosco, P. Fattori, and A. P. del Pobil. The dorso-medial visual stream: from neural activation to sensorimotor interaction. *Neurocomputing*, 74(8):1203–1212, mar 2010.
7. T. Collins, K. Dore-Mazars, and M. Lappe. Motor space structures perceptual space: Evidence from human saccadic adaptation. *Brain Res.*, 1172:32–39, August 2007.
8. J. C. Culham. Functional neuroimaging: Experimental design and analysis. In R. Cabeza and A. Kingstone, editors, *Handbook of Functional Neuroimaging of Cognition*, pages 53–82. MIT Press, Cambridge, MA, 2006.
9. P. Dario, M.C. Carrozza, E. Guglielmelli, C. Laschi, A. Menciassi, S. Micera, and F. Vecchi. Robotics as a future and emerging technology: biomimetics, cybernetics, and neuro-robotics in European projects. *IEEE Robotics & Automation Magazine*, 12(2):29–45, June 2005.
10. M. Kawato. Robotics as a tool for neuroscience - cerebellar internal models for robotics and cognition. In *Proceedings of the 9th International Symposium on Robotics research*, pages 321–328, 2000.
11. M. Lappe. What is adapted in saccadic adaptation? *J. Physiol.*, 587(Pt 1):5, 2009.
12. S. McLaughlin. Parametric adjustment in saccadic eye movements. *Percept. Psychophys.*, 2:359–362, 1967.
13. T. Nanayakkara and R. Shadmehr. Saccade adaptation in response to altered arm dynamics. *Journal of Neurophysiology*, 90(6):4016–4021, 2003.
14. T. J. Prescott, P. Redgrave, and K. Gurney. Layered control architectures in robots and vertebrates. *Adaptive Behavior*, 7(1):99–127, 1999.
15. E. Salinas and P. Thier. Gain modulation: a major computational principle of the central nervous system. *Neuron*, 27(1):15–21, July 2000.
16. F. Schnier, E. Zimmermann, and M. Lappe. Adaptation and mislocalization fields for saccadic outward adaptation in humans. *Journal of Eye Movement Research*, 3(3):1–18, 2010.
17. N.G. Tsagarakis, G. Metta, G. Sandini, D. Vernon, R. Beira, F. Becchi, L. Righetti, J. Santos-Victor, A.J. Ijspeert, M.C. Carrozza, and D.G. Caldwell. icub: the design and realization of an open humanoid platform for cognitive and neuroscience research. *Advanced Robotics*, 21(10):1151–1175, 2007.